2022-05-01

Material Synthesis and Additive Manufacturing of Ceramics

Elsa Bramasco-Rivera
The University of Texas at El Paso

Recommended Citation

Bramasco-Rivera, Elsa, "Material Synthesis and Additive Manufacturing of Ceramics" (2022). *Open Access Theses & Dissertations*. 3474.
https://scholarworks.utep.edu/open_etd/3474

MATERIAL SYNTHESIS AND ADDITIVE MANUFACTURING OF CERAMICS

ELSA BRAMASCO-RIVERA

Master’s Program in Mechanical Engineering

APPROVED:

Yirong Lin, Ph.D., Chair

Elizabeth Reza, M.S., Co-Chair

Angel Flores-Abad, Ph.D.

Stephen L. Crites, Jr., Ph.D.
Dean of the Graduate School

Dedication

To my parents, Hilda and Federico, who always gave their three daughters everything, for their support, and their endless love. To my sisters, Laura and Cecilia, for their ongoing motivation. To my second mother Elsa and my niece Daleyza for their encouragement. And to all those who always push me to keep going even when times are tough.

MATERIAL SYNTHESIS AND ADDITIVE MANUFACTURING OF CERAMICS

by

ELSA BRAMASCO-RIVERA, B.S.

THESIS

Presented to the Faculty of the Graduate School of
The University of Texas at El Paso
in Partial Fulfillment
of the Requirements
for the Degree of

MASTER OF SCIENCE

Department of Mechanical Engineering
THE UNIVERSITY OF TEXAS AT EL PASO
May 2022

Acknowledgements

I would first like to thank my advisor Dr. Lin for his continued guidance over the past almost three years. Dr. Lin has helped me become a better professional in my field by providing me the necessary resources to expand my knowledge and experience. I would also like to thank Dr. Sabrina Torres and Elizabeth Reza for helping me with my project and providing feedback during our monthly meetings. Also, I would like to thank Dr. Flores-Abad for being a member of my committee, along with Dr. Lin and Elizabeth Reza.

I would like to thank the University of Texas at El Paso and the Department of Mechanical Engineering for helping me become successful in the professional world. I would also like to thank the NASA Center for Space Exploration and Technology Research (cSETR, Aerospace Center), W.M. Keck Center for 3D Innovation, Kansas City National Security Campus, and MSIPP for allowing me to conduct my research.

I would like to thank all my lab mates in the Smart Materials Printing Lab, especially Jaime, who has been my mentor and friend since my entry to the group. Thanks to Sebastian, Andrea, and Joshua for making working in the lab a fun experience. Lastly, I would like to thank my close friends Bryan, Ferrant, and Oscar for making the past six years of university fun and for always being there when I needed them, including when working together in the lab.

Abstract

This research is divided into two main topics: vitrimer polymers and alumina ceramics. Additive manufacturing is an emerging technology. In this research, two main methods of additive manufacturing are used: material extrusion and vat photopolymerization. The hypothesis of self-healing and mechanochromism functionalities was tested through the synthesis of vitrimers, a novel material combining properties of both thermosets and thermoplastics. These vitrimers were 3D printed using material extrusion. Casted vitrimers showed stiffening effects after submergence in water. Lithography based ceramics have gained attention in recent years due to their wide range of applications. Alumina ceramics were additively manufactured using digital light processing. Sintering of parts showed a shrinkage of 14%. Scanning electron microscopy images revealed a dense microstructure. Density proved to be 3.82 g/cm^3, achieving about 99% of theoretical density. Additional research was conducted reducing graphene oxide to have similar properties to graphene, which was then used in a commercial resin to 3D print plastic parts using stereolithography.

Table of Contents

List of Tables

List of Figures

List of Illustrations

Introduction

Additive manufacturing (AM), also known as 3D printing, is the process of joining materials to make parts from 3D model data, usually layer upon layer, as opposed to subtractive manufacturing and formative manufacturing methodologies [1]. This type of manufacturing is divided into seven categories: material extrusion, vat photopolymerization, powder bed fusion, binder jetting, material jetting, sheet lamination, and directed energy deposition. However, the two methods of focus here are material extrusion and vat photopolymerization. Material extrusion is the process in which material is selectively dispensed through a nozzle or orifice. Vat photopolymerization is the process in which liquid photopolymer in a vat is selectively cured by light-activated polymerization [1].

Advantages of additive manufacturing include being able to create complex geometries. Due to the capabilities of the different AM technologies, intricate designs can be created. Since parts can be printed at a fast pace, rapid prototyping can be achieved, where for example, other types of manufacturing methods may require the use of molds, which take a lot of time to create. There is low material waste due to depositing only the necessary material onto a part, which in turn reduces and/or eliminates tooling costs. Finally, 3D printing allows full customization; if a part needs fixing after printing, it can rapidly be redesigned and be printed again [2].

However, there are some limitations to additive manufacturing, including high costs. Though some 3D printers can be inexpensive of only a few hundred dollars, others can cost up to hundreds of thousands of dollars, depending on the technology being used. Post-processing may be necessary, depending on the printed outcome. Although some machines can be large, there may be a restricted build size, which is the only section that can produce the printing. These build sizes can be restricted to only a few millimeters in the x, y, and z directions. Some geometries may require support structures to assist during the printing process, where angles less than 35° will require supports, which will need to be removed after printing. These supports can leave some markings at the interface of the printed structure and the support, which is oftentimes unwanted. Surface finishes may be rough and may require some type of post-processing. For example, plastics manufactured using material extrusion oftentimes have a rough surface, showing the nozzle diameter used to print it, and may undergo vapor smoothing to smooth the surface. Finally, time is another issue with additive manufacturing. Though some prints may require a few minutes to print, others can take several hours, to days, to even a full week [3],[4].

Both advantages and disadvantages depend on the type of technology of additive manufacturing used.

Illustration 1.1: The seven categories of additive manufacturing.

Material Synthesis

Chapter 1: Vitrimers

1.1 INTRODUCTION

About 380 million tons of plastic are produced each year, of which only about 8-10% is successfully recycled [5]. There are two types of plastics: thermosets and thermoplastics. Thermosets do not soften and retain their shape when heated. They are harder and stronger than thermoplastics and have excellent strength attributes. Thermosets cannot be recycled because they are chemically joined by strong covalent crosslinks [6]. Thermosets include polyester resins [7], polyurethanes [8], and vulcanized rubber [9]. On the contrary, thermoplastics soften and can be reshaped when heated. They can be recycled because their molecules are not chemically joined together. Instead, they are joined by hydrogen bonds or intermolecular forces, such as Van der Waals. Thermoplastics can be heated and cooled several times without changing their chemical or mechanical properties [10]. Thermoplastics include polyethylene [11], polypropylene [12], and polyvinyl chloride [13].

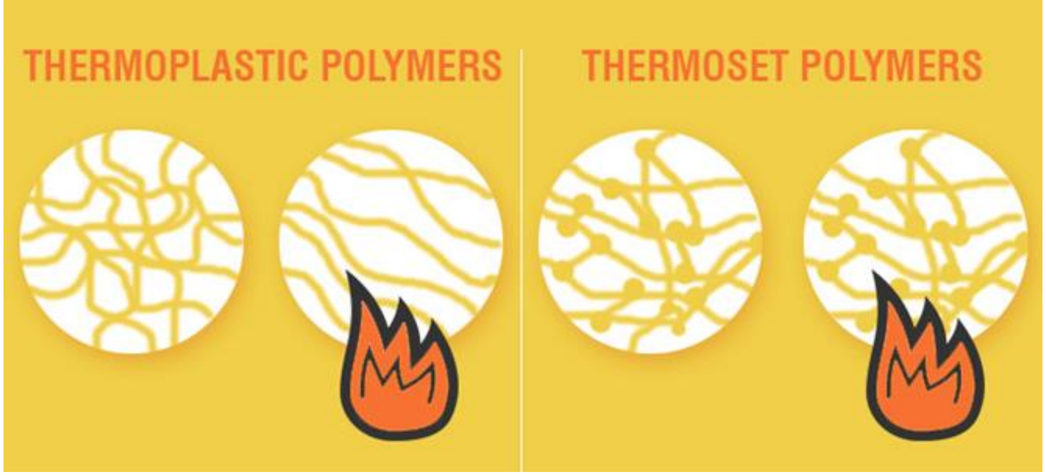

Figure 1.1: Chemical bonds of thermoplastic and thermoset polymers.
https://www.ozseals.com/thermoplastic-vs-thermoset-whats-the-difference/

1.2 BACKGROUND AND MOTIVATION

Since there exists a lot of plastic waste that affects the environment, alternatives must be found. Leibler and co-workers [14] discovered vitrimers, a new novel material that contains characteristics of the both types of plastics. Vitrimers are joined by strong covalent networks like thermosets but can be reshaped and recycled like thermoplastics. Vitrimers contain covalent adaptive networks, allowing their desired properties.

Materials with covalent adaptive networks are thermosets with dynamic crosslinkers inside, which are reversible covalent bonds. These reversible covalent bonds enable the crosslinked structure to respond chemically to an applied stimulus, which allow reshapability, recyclability and shape memory [15]. The addition of dynamic crosslinkers in the network allow material to flow like a thermoplastic [16]. Bonds exchange when heated, allowing the reshapability. Since the number of bonds remains constant, the polymer will not dissolve [17]. A type of chemistry that allows vitrimers to have its desired properties is disulfide exchange, a chemistry that undergoes a radical mediated mechanism [18]. This type of exchange occurs at lower temperatures and faster than other types of reactions, such as coordination bonds [19] and Diels-Alder [20].

Thermoplastics only contain a glass transition, the temperature at which a material goes from a glassy state to a rubbery state [21]. Vitrimers, however possess a second transition: the topology freezing transition temperature, Tv, which shows a change from a viscoelastic solid to a viscoelastic liquid, indicating when the vitrimer becomes processable. This second transition is due to exchange reactions occurring [22].

1.3 VITRIMER SYNTHESIS

Vitrimer synthesis was completed for 3D printing. First, the preparation of self-sensing polymer composites was fabricated.

Materials

Bisphenol A diglycidyl ether (BPA) (340.41 g/mol) was purchased from Sigma Aldrich (Darmstadt, Germany). 2-Aminophenyl disulfide, 2-AFD, (248.37 g/mol) and 4-Aminophenyl disulfide, 4-AFD, (248.37 g/mol) were purchased from Sigma Aldrich as well. Graphene oxide (GO) in the suspension of 5 g/mL was purchased from Goographene (Fairfax, Virginia, United States).

Methodology

To prepare the BPA/2-AFD vitrimer, bisphenol A diglycidyl ether was melted at 85 °C. 2-Aminophenyl disulfide was added and stirred for 15 minutes. Same process was used for the BPA/4-AFD vitrimer. BPA/2-AFD/GO vitrimer was prepared using the same process, but graphene oxide was added at the beginning, stirred for 15 minutes, followed by the addition of the 2-aminophenyl disulfide.

Results

BPA/2-AFD vitrimer exhibited self-healing properties, while BPA/4-AFD vitrimer exhibited transient mechanochromism, meaning there is a change in color in response to mechanical damage. After scratching this vitrimer against sandpaper, the surface changes to a green color, as seen in figure 1.2. The addition of graphene oxide was used to increase toughness of the BPA/2-AFD vitrimer. Upon using a needle to create a deep scratch onto the material and healing at 180 °C after five minutes under mild pressure, the fractured surface heals itself, however, there is a rough surface that remains as can be seen in figure 1.3.

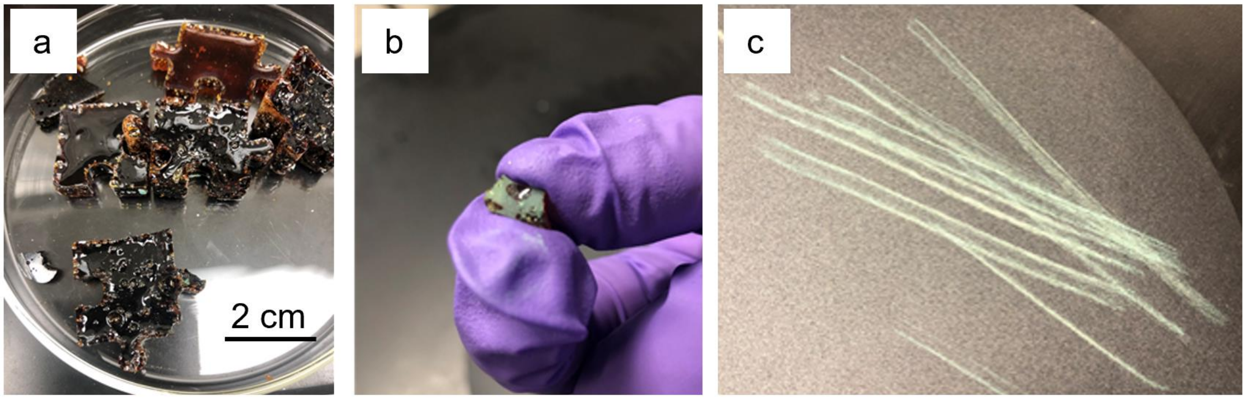

Figure 1.2: BPA/4-AFD vitrimer showing mechanochromism.

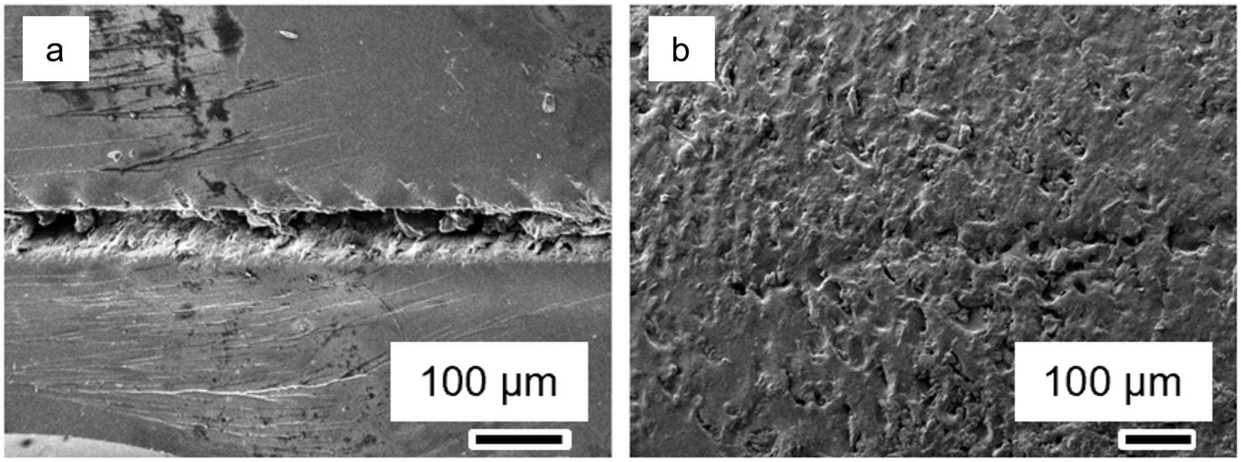

Figure 1.3: BPA/2-AFD/GO vitrimer. a) Fractured surface, b) Healed surface.

Thermogravimetric analysis showed the degradation of the BPA/2-AFD/GO vitrimer at 315 °C, showing that it can be safely re-healed at 180 °C, since there is no reaching of such a high temperature.

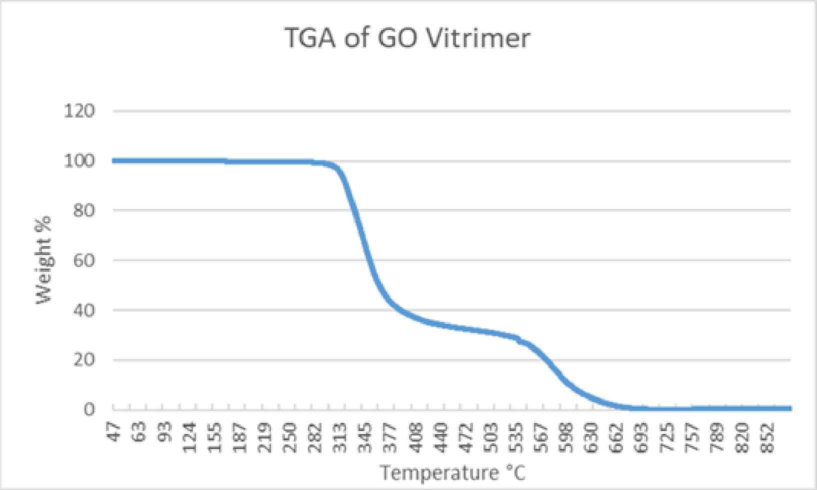

Figure 1.4: Thermogravimetric analysis of BPA/2-AFD/GO vitrimer.

Conclusion

Using disulfide chemistry in vitrimers gives them their characteristics. In this case, vitrimers show transient mechanochromism, changing color upon stresses, and self-healing characteristics through an external stimulus. Applications include structural components in automotive or aeronautics where a damaged part can be detected easily and the part can heal itself using an external stimulus such as heat or pressure, or both.

Table 1.1: Summary of Vitrimer Properties.

Vitrimer	Properties
BPA/2-AFD	Self-healing
BPA/4-AFD	Mechanochromism
BPA/2-AFD/GO	Self-healing, Cures faster

1.4 VITRIMER PRINTING

After characterization of self-sensing composites, printing was achievable.

Methodology

Material extrusion Hyrel Engine HR (Norcross, Georgia, United States) 3D printer was used. Vitrimer was extruded using a 0.8-millimeter nozzle, down to the smallest diameter of 0.2 millimeters.

Results

The BPA/2-AFD vitrimer was extruded at 80 °C and reused for up to two months where towards the end of its life, it obtained a rubbery consistency that required much higher temperatures to print, which can lead to final curing of the material that is no longer malleable or able to flow.

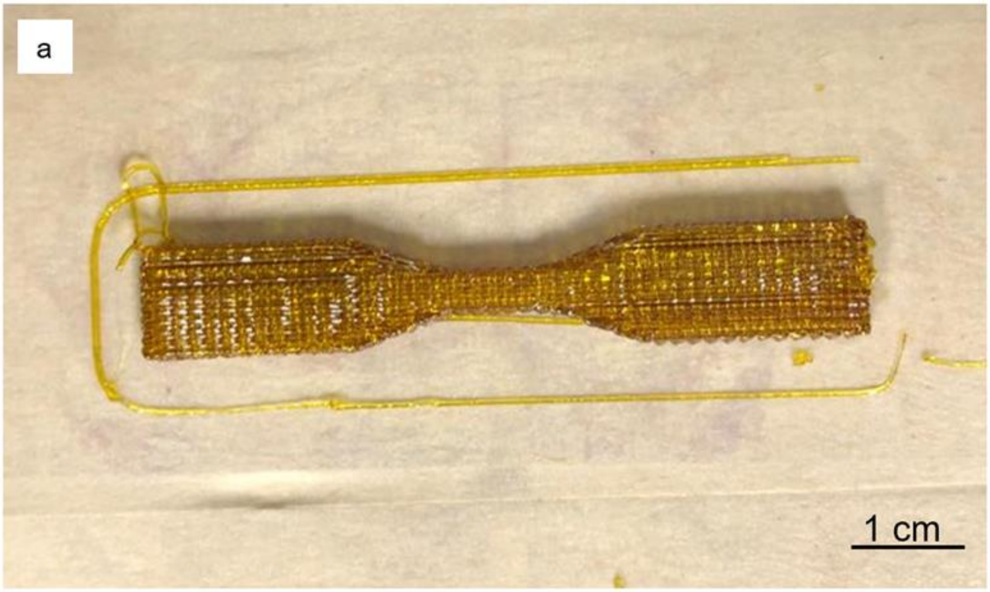

Figure 1.5: BPA/2-AFD printed vitrimer (dog bone geometry).

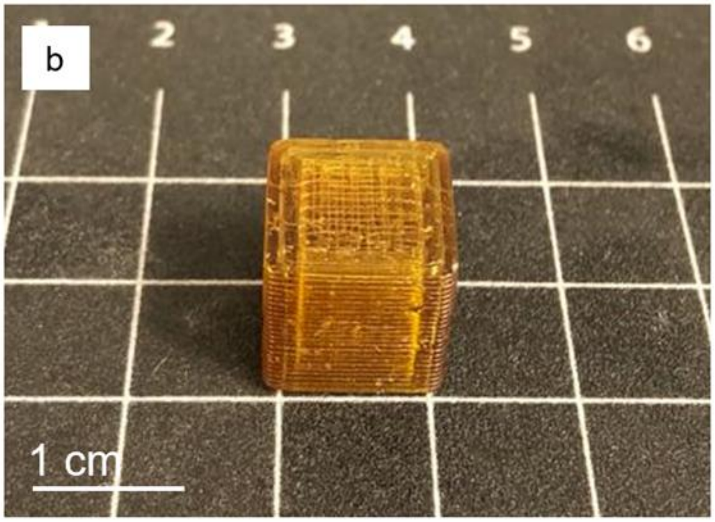

Figure 1.6: BPA/2-AFD printed vitrimer (cube geometry).

The BPA/2-AFD vitrimer became brittle after printing, making it difficult to remove from the build plate, as this led to cracking and even complete breaking. To help with printing, graphene oxide and polyethylene glycol (PEG) were added to the synthesis of the BPA/2-AFD vitrimer. Graphene oxide increases toughness, while polyethylene glycol behaves as a plasticizer and retardant, preventing complete crosslinking and avoiding the rubbery consistency that increases difficulty of printing. This BPA/2-AFD/GO/PEG vitrimer was printed at 90 °C and contained good recyclability for printing.

Figure 1.7: BPA/2-AFD/GO printed vitrimer.

Conclusion

Vitrimer printing is achieved using material extrusion additive manufacturing technologies. It is important to print using temperatures below the curing temperature to achieve a processable material that is capable of flowing. As pure vitrimer can be brittle after printing, it requires the use of additives incorporated into the material. Additives used here include graphene oxide to increase toughness and polyethylene glycol, which acts as a plasticizer and retardant to prevent further crosslinking, preventing complete curing of the material. Specimens were printed using the smallest diameter of 0.2 millimeters.

1.5 WATER-INDUCED STIFFENING EFFECTS ON VITRIMER

Water was used as a hypothesis to remove polyethylene glycol to help with processing. Upon addition of water, some unexpected effects were discovered.

Methodology

Bisphenol A diglycidyl ether was melted at 85 °C. 2-Aminophenyl disulfide was added and stirred for 15 minutes. Polyethylene glycol (PEG400) purchased from Sigma Aldrich was then added and stirred for an additional 15 minutes. Finally, samples were casted in silicon molds and cured for 20 hours at 150 °C.

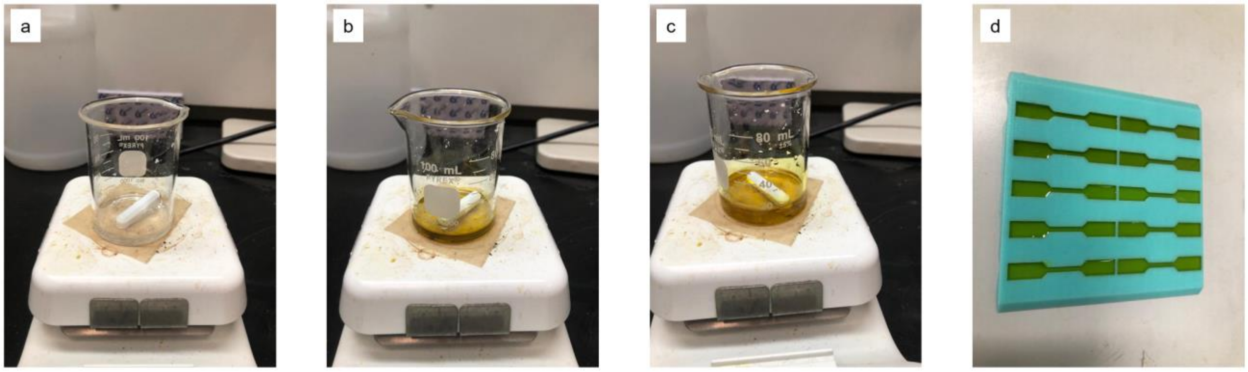

Figure 1.8: Methodology for water-induced stiffening vitrimer. a) BPA is melted, b) 2-Aminophenyl disulfide is added, c) Polyethylene glycol is added, d) Samples are casted and cured for 20 hours.

Results

Casted samples have a soft, flexible feeling. After being submerged in water at room temperature, the vitrimer stiffens and is no longer flexible. This can be reversible up to a certain time of these parts being submerged in water. However, further research must be done to characterize the threshold where parts do not go back to a soft texture. These BPA/2-AFD/PEG casted vitrimers also contain shape memory.

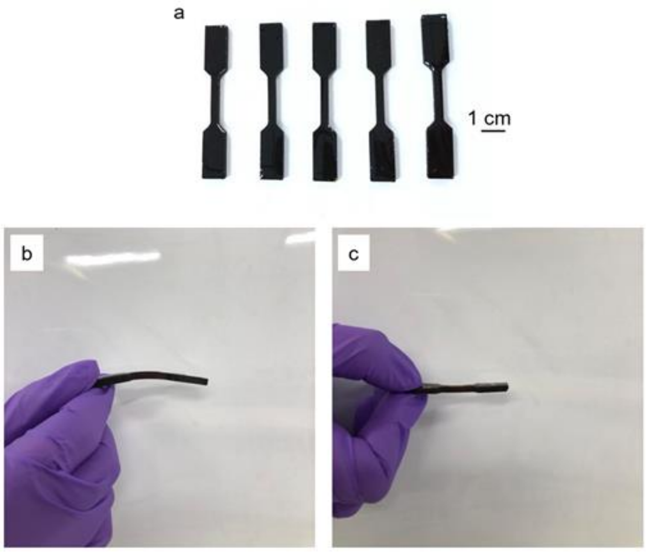

Figure 1.9: a) Casted BPA/2-AFD/PEG samples, b) Soft sample, c) Water-stiffened sample.

Mechanical testing was completed by conducting tensile testing according to ASTM D638 standard used for polymers. There is a 585x modulus increase from a dry-casted sample to a water-stiffened sample. Dry samples exhibit elastomer-like behavior, and wet-treated samples become tough.

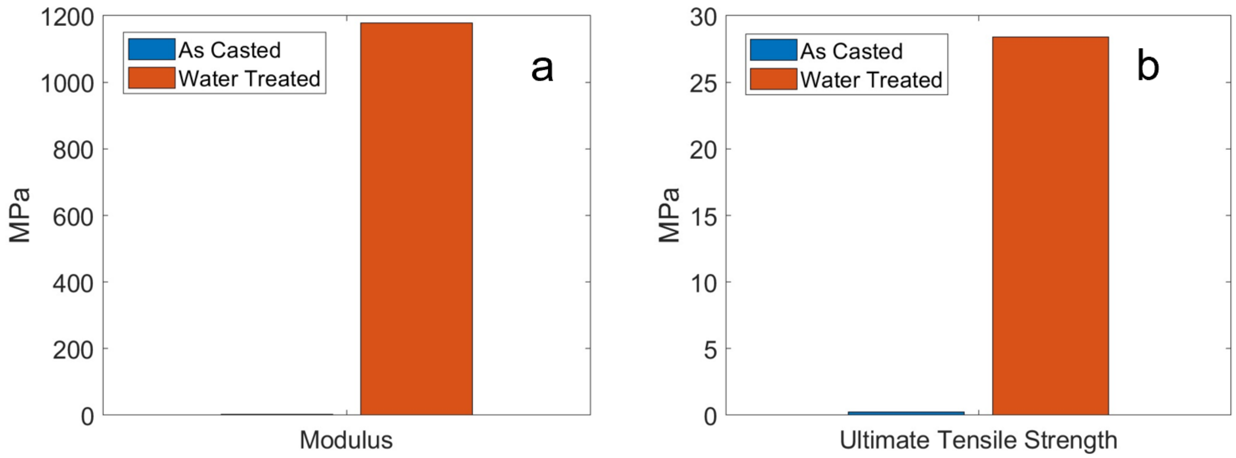

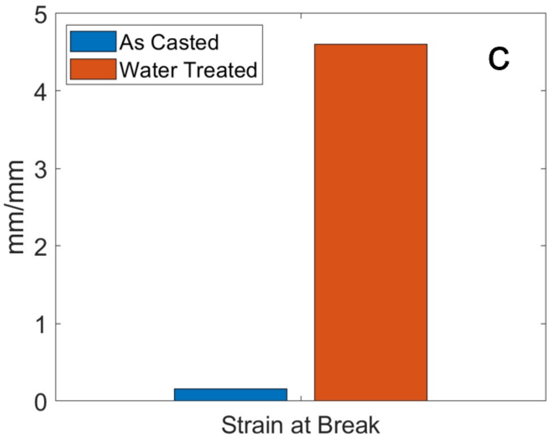

Figure 1.10: Mechanical testing of water-stiffened vitrimer. a) Modulus, b) Ultimate tensile strength, c) Strain at break.

X-ray diffraction (XRD) shows changes in crystalline structure. There is a loss of amorphous structure, which shows a phase separation and movement of polyethylene glycol from the surface. Polyethylene glycol blocks crosslinking, and partially cured vitrimer gets triggered when water moves the polyethylene glycol.

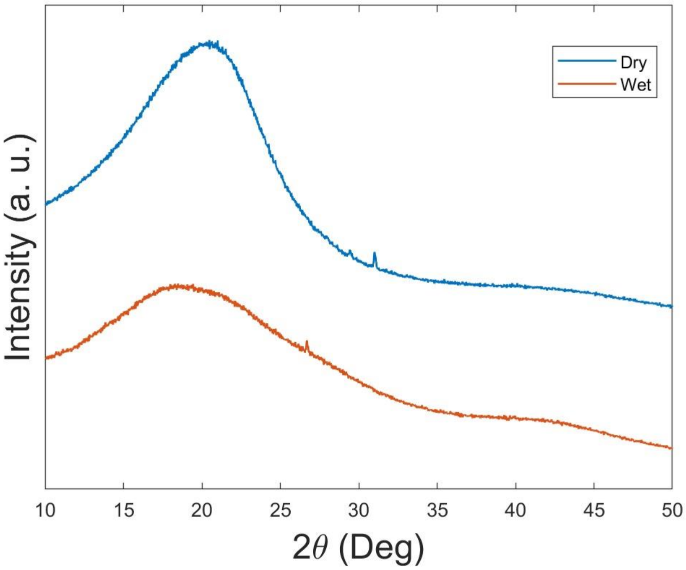

Figure 1.11: X-ray diffraction of water-stiffened vitrimer. Dry samples are as-casted samples. Wet samples are water-treated samples.

Conclusion

Casted samples composed of monomer bisphenol A diglycidyl ether, hardener 2-aminophenyl disulfide, and retardant polyethylene glycol exhibited water-stiffening effects after submergence in room temperature water. Water-treated samples show a 585x modulus increase when compared to dry, casted samples. The ultimate tensile stress of water-treated samples is almost 30 MPa, while that of casted samples is less than one MPa. There is a phase separation between hydrophobic epoxy and hydrophilic polyethylene glycol allowing these effects to occur. Applications of these materials include soft robotics due to their shape memory and structural components due to their strength.

Future Work

As previously mentioned, characterization of the threshold at which the polymer is no longer reversible from a stiffened water-treated sample back to a soft material must be completed. This is to further detect the amount of time that affects this reversibility phenomenon.

Additive Manufacturing of Ceramics

Chapter 2: Alumina Ceramics

2.1 INTRODUCTION

Alumina (Al_2O_3), also known as aluminum oxide is a popular engineering material, a crystalline substance, commonly used for its physical and chemical stability [23]. Alumina is inexpensive for an advanced ceramic, with great thermal, chemical and mechanical properties, compared to other much more expensive materials [24]. It is made from a very fine silky white granular material, processed from bauxite, an aluminum-rich material found in the Earth's crust [25]. Alumina ceramics possess resistance to strong acids at high temperatures because they are inert, meaning they are not chemically reactive. Alumina as a ceramic has high strength and stiffness due to its hardness. Alumina ceramics possess good abrasion and wear resistance, electrical resistivity [23], high thermal conductivity, electrical insulation, corrosion resistance, high temperature oxidation resistance, and outstanding biocompatibility [25]. Contrary to metals which weaken at high temperatures, alumina ceramics retain their strength after returning to normal temperatures, and are stronger than some types of stainless steels [23]. Alumina ceramics can be used in several applications, including medical, electronics, dentistry, automotive, and aerospace.

2.2 BACKGROUND AND MOTIVATION

Alumina was unknown until after World War II, when the alumina ceramics industry began around the year 1950 [25]. However, since then, alumina ceramics can now be seen in a wide range of applications, including live-saving and life-enhancing technologies. Cardiac pacemakers contain an alumina feedthrough, keeping those that suffer from arrythmia alive [25]. Alumina bearings are used in hip replacement implants. Lightweight alumina body armor was first used in

1965, but became a military secret until the 1990s, where today alumina can be seen in infantry and law enforcement applications, both as body armor and vehicle armor [25]. Due to its high thermal conductivity and electrical insulation properties, alumina is a great heatsinking insulator for microchips, microsensors, and microelectronics [25]. Dental applications of alumina include dental crowns, bridges, and implants [25]. Chemical alumina is powdered alumina used in catalysts, polishing powders, alumina cements, and as an additive to create high-purity alumina ceramics, such as those in this research [25].

Figure 2.1: Alumina zirconia toughened (AZT) ball-socket hip replacement. [25]

Figure 2.2: Alumina-fiberglass ceramic body amor used in the 1980s. [25]

Figure 2.3: Alumina parts. https://precision-ceramics.com/materials/alumina/

Creation of alumina ceramics is divided into three categories: wet forming, dry forming, and additive manufacturing (AM) [25]. Wet forming is the original process of ceramic production, having the advantage of being able to achieve shape complexity, but the disadvantage of needing drying [25]. Dry forming is a simple and fast mass production process having the advantage of not requiring drying, but the disadvantage of not achieving shape complexity [25]. As expected, wet forming and dry forming are opposites of each other. Finally, as previously mentioned, additive manufacturing adds material to create final parts, having the advantage of being able to achieve complex shapes, but the disadvantage of needing drying [25].

There are two main wet forming methods: powder injection molding and tape casting [25]. Powder injection molding is a highly expensive process only used for complex shapes with high precision when cost is not an important factor to consider. Powder injection molding is the process of preparing a feedstock, granulating into pellets, and feeding these pellets into an injection molding machine. Granulated feedstocks are then heated to form a flowable paste, followed by injection into a mold under high pressure. Parts are cooled and removed from the molds, followed by debinding and sintering. However, binder removal is problematic as it may require chemical or thermal methods, or sometimes both. Tape casting is frequently seen in the electronics industry as it is typically used for creating thin films. Tape casting involves the formation of thin sheets of ceramics by feeding a slurry through a blade that is then rapidly dried by evaporation [25]. In wet forming methods, since drying is required, other factors must be considered, including shrinkage problems, energy costs, time, and cracking risks.

The two main dry forming methods are uniaxial die pressing and cold isostatic pressing [25]. Uniaxial die pressing is used for easy prototyping and mass production of simple parts. Uniaxial die pressing involves the feeding of dry powders with very minimal binders and liquids into a uniaxial hollow die, such as pressing plates or pistons, that apply pressure to form the fed powder into a ceramic component, followed by debinding and sintering [25]. Due to pressure gradients during pressing, there can exist nonuniform particle packing. Uniaxial die pressing is ideal for simple flat components such as mosaic tiles seen in homes. Cold isostatic pressing is used when complex shapes are desired, but injection molding is not an option for whatever reason. Through cold isostatic pressing, a ceramic powder is placed in a thin-walled mold that is then immersed in an oil chamber and pressurized. This method uses more uniform pressing than uniaxial die pressing because pressing occurs in all directions in three dimensions. Since dry forming does not require the need for drying, the previous problems mentioned seen in wet forming are avoided.

Currently, there are two main additive manufacturing methods to fabricate alumina ceramics: material jetting and powder bed fusion [25]. In material jetting, droplets of build are jetted onto a build platform and cured with heat or a UV source. Powder bed fusion uses a laser or electron beam to fuse materials together. However, these two methods can be highly expensive processes used for short production runs.

2.3 HIGH PURITY ALUMINA CERAMICS

Injection molding and pressing require special dies, time, labor, and machining costs. Special molds to design ceramics are highly expensive. If ceramics can be printed directly, money, time, and labor can be saved. Therefore, the objective of this research is to show the printing capabilities of alumina ceramics using digital light processing (DLP) additive manufacturing. DLP is a process in which a 3D object is created using UV light. At the bottom of the printer there is a UV projector that projects light onto the resin vat above it. This vat contains the photopolymer resin. Each projection of light creates a new layer. As the part is printed, the build plate moves upwards, allowing the part to continue to be printed.

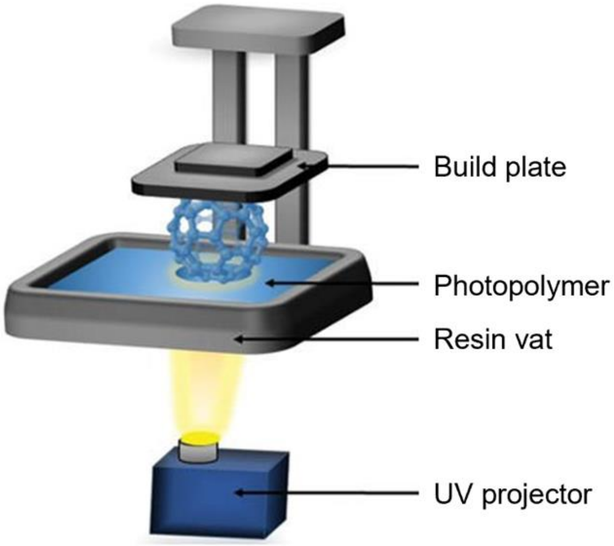

Figure 2.4: Schematic of digital light processing additive manufacturing.

Materials

The printer used is a Bison 1000 DLP printer by Tethon 3D (Omaha, Nebraska, United States). The Bison 1000 features x and y resolutions of 57 microns, z resolution of 25 microns, and a build size of 110 x 60 x 138 millimeters. The projector uses a 405 nanometer UV LED light. The resin used is a high purity alumina (HPA) resin, a commercial photosensitive resin with 99.8% alumina, also from Tethon 3D (Omaha, Nebraska, United States).

Methodology

A 3D model is first designed using 3D model software, a combination of SolidWorks, Autodesk Fusion 360, and/or nTopology. The design is imported into the printer where it is left to print. After the part is finished, it is washed with isopropanol to get rid of any uncured resin left on the part. It then goes through a second curing under a 405 nanometer UV light. Finally, the part is sintered in a furnace.

Figure 2.5: Methodology for alumina ceramics additive manufacturing. [26]

Table 2.1: High Purity Alumina Sintering Schedule.

Step	Rate (°C/min)	Temperature (°C)	Hold (hr)
1	7	1625	6
2	Natural cool down		

Results

First, a resin validation matrix is printed. This is a test design typically used for photopolymer resins to evaluate printing parameters and tells the user whether exposure times must be increased or decreased depending on undercuring or overcuring happening. The printing parameters used consisted of an initial exposure time of 275 seconds, meaning that to print the initial four layers, it takes 275 seconds to cure each layer. The remaining layers were each cured at a basic exposure time of 250 seconds. Upon printing and sintering, the part experiences an overall shrinkage of 13.69%. The manufacturer claims shrinkage should be around 14%, showing effective sintering of these printed parts. After sintering, the most important parameter is density. Before sintering, in the green state, the part has a density of 2.81 g/cm³ and after sintering it increases to 3.81 g/cm³, achieving approximately 99% of theoretical density.

Figure 2.6: Printed and UV cured HPA showing overexposure.

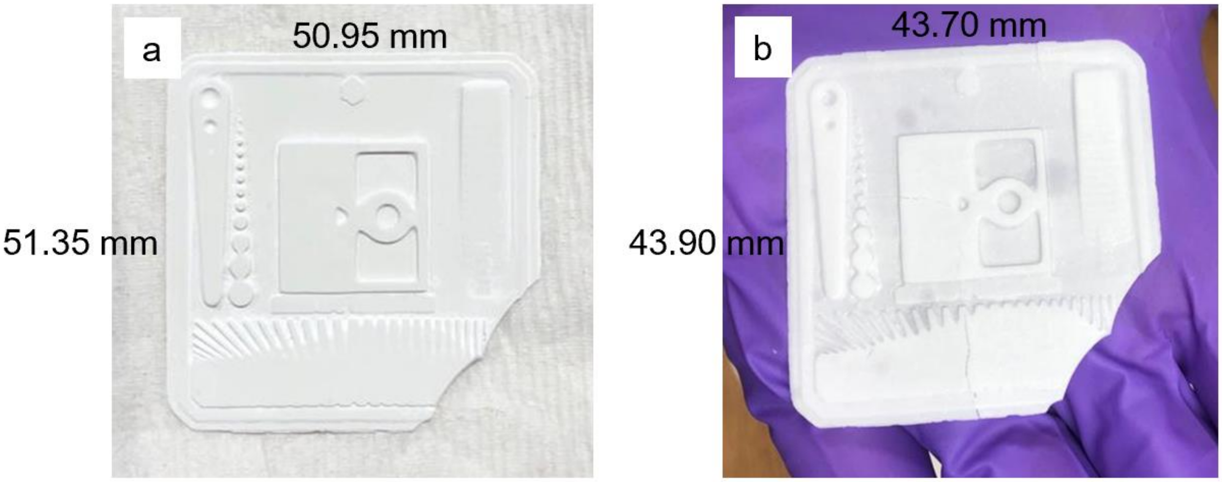

Figure 2.7: Resin validation matrices with measurements. a) Pre-sintered part, b) Sintered part.

Table 2.2: Shrinkage for Resin Validation Matrix.

X-Direction	14.23%
Y-Direction	14.37%
Z-Direction	12.46%
Overall Shrinkage	13.69%

Scanning electron microscopy (SEM) images of the resin validation matrix were taken pre-sintering and post-sintering. In the top view of the green state, the silky white powder of alumina previously mentioned is seen, where after sintering, there is more of a homogeneous densification.

In the SEM images of the bottom surface of the resin validation matrix, the green part again shows the powder as expected, and on the sintered part densification is seen. However, some cracks are visible as well, and these are due to friction that occurs between the bottom surface of the part and the crucible used where the part is placed during sintering. There are also some blobs visible, and these are attributed to an adhesive used on the build plate for parts to stick to it and not fall throughout the printing process. Cross section SEM images of the parts show the change from the powdery material to a dense material; however, some cracks are seen as well. The cracks in the cross section are attributed to uncured resin left in the green part that was not properly removed during the isopropanol wash. Uncured resin left behind can affect sintering of parts as seen in these formed cracks, which is why it is important for the parts to be deeply cleaned.

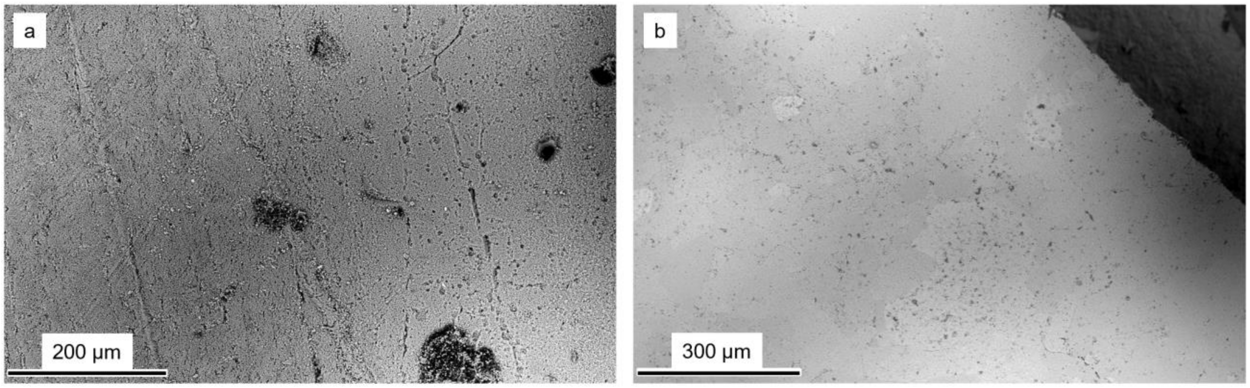

Figure 2.8: Scanning electron microscopy of the top surface of the resin validation matrix. a) Pre-sintered part, b) Post-sintered part.

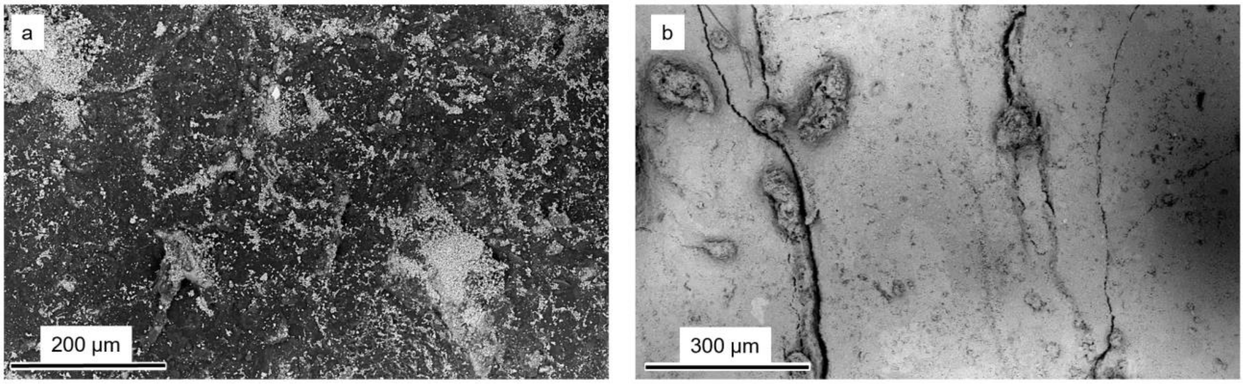

Figure 2.9: Scanning electron microscopy of the bottom surface of the resin validation matrix. a) Pre-sintered part, b) Post-sintered part.

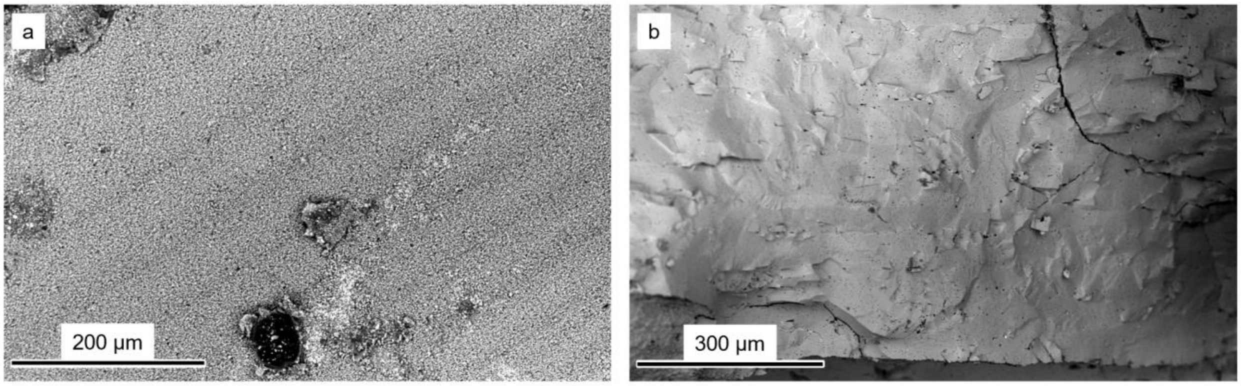

Figure 2.10: Scanning electron microscopy of the cross section of the resin validation matrix. a) Pre-sintered part, b) Post-sintered part.

To further characterize shrinkage and density measurements of the high purity alumina ceramic prints, other geometries were printed as well, including a columnar lattice, heat sink, and gyroid pyramid. The columnar lattice showed an overall shrinkage of 13.43%, the heat sink of 15.51%, and the gyroid pyramid of 14.51%, averaging 14.49%, still being in the 14% regime.

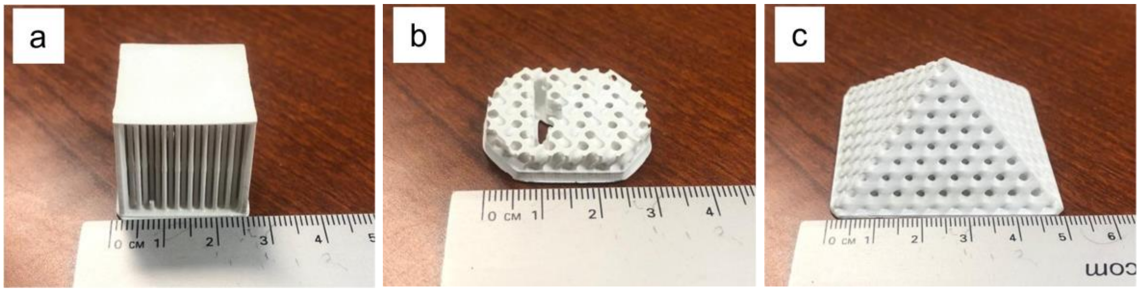

Figure 2.11: Other printed alumina ceramic geometries. a) Columnar lattice, b) Heat sink, c) Gyroid pyramid.

Table 2.3: Shrinkage of Parts.

Shrinkage (%)	Columnar Lattice	Heat Sink	Gyroid Pyramid
X-Direction	10.03	14.97	13.88
Y-Direction	14.75	15.81	13.70
Z-Direction	15.51	15.76	15.96
Overall Shrinkage	13.43	15.51	14.51
Average Shrinkage: 14.49			

Table 2.4: Densities Pre-Sintering and Post-Sintering.

	Columnar Lattice	Heat Sink	Gyroid Pyramid
Density Before Sintering (g/cm^3)	2.13	2.48	2.73
Density After Sintering (g/cm^3)	3.87	3.81	3.77

X-ray diffraction was conducted to see any changes before and after sintering. However, the same peaks are seen pre-sintering and post-sintering, showing no change in crystallographic structure, while also showing no decomposition, breakage, or phase separation. The XRD also matches with XRD of other alumina ceramics in literature.

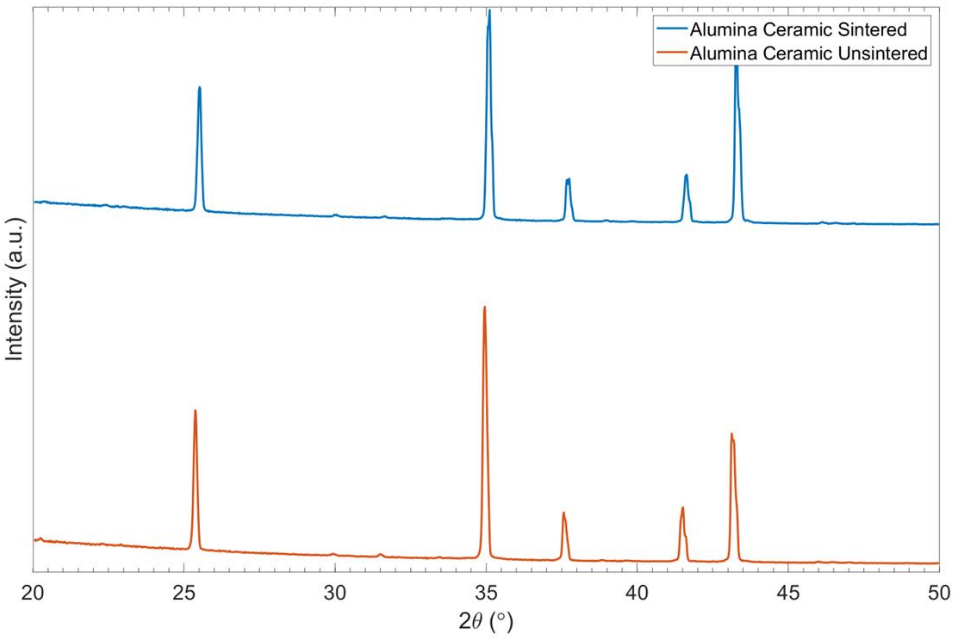

Figure 2.12: X-ray diffraction of printed alumina ceramic parts.

Lessons Learned and Challenges

Regarding lessons learned and challenges, printing can be difficult as prints can require several iterations. This is until the optimal printing parameters are found, though. Once these have been found, the user sets a printer to print and just lets it print for the time required. Parts can stick to the build plate, which is something desired to avoid any falling throughout the printing process. However, when parts are too stuck, it can be difficult to remove the prints and can lead to cracking or breaking during removal from the build plate, also showing the delicacy of green parts, so they must be removed with care. Support structures may be necessary, an addition to the handling with care needed to remove them. There are limitations in wall thickness due to the expected shrinkage to occur. If walls are too thin, they can crack or even break. The overall printing process may take several days, but this is due to the iterations required to find the optimal printing parameters. Finally, cleaning can take a lot of time and is a messy process because a liquid resin is used and since it is recycled, it must be filtered through a sieve to eliminate any pieces of cured resin left behind. Once, the resin has been filtered, it is reused for the next print.

2.4 CONCLUSION

Overall, 3D printing of alumina ceramics is achievable using digital light processing additive manufacturing. This method saves time, labor, and costs when compared to other types of alumina ceramics manufacturing methods. There is a predictable shrinkage of 14% expected to occur after the sintering process. Parts have good surface quality that can be differentiated from other types of additive manufacturing technologies where for example, after using material extrusion, rough surfaces are seen. Average density of parts is 3.82 g/cm³, achieving about 99% of theoretical density. Printing parameters of parts depends on the complexity of designs where the columnar lattice, heat sink, and gyroid pyramid require an initial exposure time of 360 seconds and a basic exposure time of 345 seconds, while the resin validation matrix requires an initial exposure time of 275 seconds and a basic exposure time of 250 seconds. Applications for these alumina ceramics include electronics, aerospace, dentistry, medical, and automotive industries. Using additive manufacturing allows small channels such as those seen in the gyroid pyramid, which allow efficient heat dissipation.

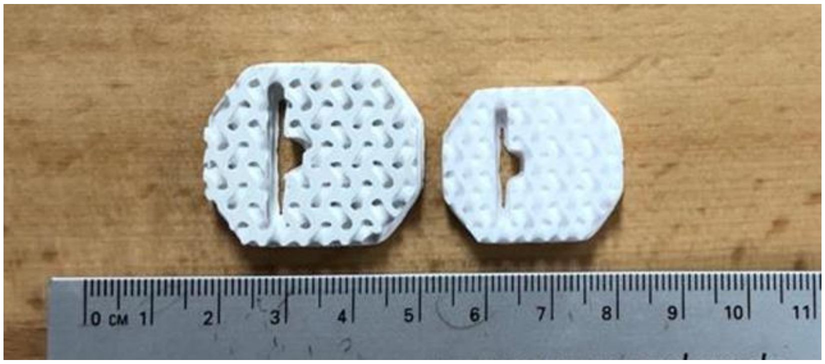

Figure 2.13: Heat sink showing predictable 14% shrinkage. Left larger part is pre-sintered. Right smaller part is sintered.

2.5 FUTURE WORK

Future work of alumina ceramics using digital light processing includes manufacturing lattice structures, an architecture formed by unit cells with faces and edges [27]. Both destructive and nondestructive testing such as mechanical testing and thermal conductivity testing will be conducted on these lattice structures. The few previous research done on alumina ceramics using DLP by other researchers include printing lattices with diamond structure, simple cubic, body-centered cubic and face-centered cubic structures, where the lattices with the simple cubic structure exhibited the highest compressive strength and absorbed the most energy [28]. Other lattices manufactured by DLP have been used in heat exchanger design, using a Kelvin cell structure [29]. Glass ceramics that are optically transparent will also be printed using DLP to be used for microfluidics [30]. Both lattice structures and optically transparent structures are an ongoing work.

Additional Research

Chapter 3: Co-Authored Publication: Near-UV Light Assisted Green Reduction of Graphene Oxide Films Through L-Ascorbic Acid

3.1 INTRODUCTION

Graphene has been studied for energy storage devices due to its optical transmittance, high surface area, high modulus of elasticity, thermal conductivity, and electron mobility [31]. Past methods to produce graphene include liquid phase exfoliation, chemical vapor deposition, and mechanical exfoliation. However, these methods limit graphene's commercial applications due to their low scalability and high cost [32]. Therefore, one of the most researched and common methods of production is the reduction of graphene oxide (GO), which has a large scalability and a variety of methods to do so [32].

3.2 BACKGROUND AND MOTIVATION

The reduction of graphene oxide to have similar properties to graphene can be done using various methods. However, using a chemical reduction process is the most ideal process. One of the most common ways of reducing graphene oxide is by oxidizing graphite using an acidic mixture [33]. The most popularly used chemical reductant is hydrazine (N_2H_4), but it possesses several toxic effects on the environment [34]. Therefore, an environment-friendly alternative chemical reductant is required. These alternatives include sugars, proteins, organic acids, and plant extracts. Nonetheless, using these safer alternatives have not proven to produce the same quality of reduced GO as that reduced with hydrazine. GO reduction efficiency and quality comparable to hydrazine include those reduced with baker's yeast, glucose, starch-based materials, and l-ascorbic acid [32].

L-ascorbic acid (L-AA) contains anti-oxidative characteristics, while being abundant. Therefore L-AA is a green and inexpensive alternative to hydrazine. L-AA has been proven to be photosensitive in the ultraviolet spectrum [35], further enabling the capability of reducing graphene oxide, due to varying parameters such as wavelength and radiation type. In this research, the effects of near ultraviolet (NUV) light on the reductive behavior and quality of L-AA in graphene oxide films are investigated.

3.3 REDUCTION OF GRAPHENE OXIDE

Materials

Materials used include graphene oxide purchased from Goographene (Virginia, United States), L-ascorbic acid purchased from Sigma Aldrich (Darmstadt, Germany), and deionized (DI) water.

Methodology

Fifteen milliliters of graphene oxide were drop-casted onto a glass substrate and dried overnight at room temperature in air. A solution of 20 milliliters of DI water and 5 grams of L-AA were pipetted onto the GO films and left drenching for different time periods. The GO films with L-AA solution were irradiated with 405 nanometer wavelength NUV light for different time periods. L-AA was removed from the GO films using DI water. GO films were dried overnight at room temperature in air.

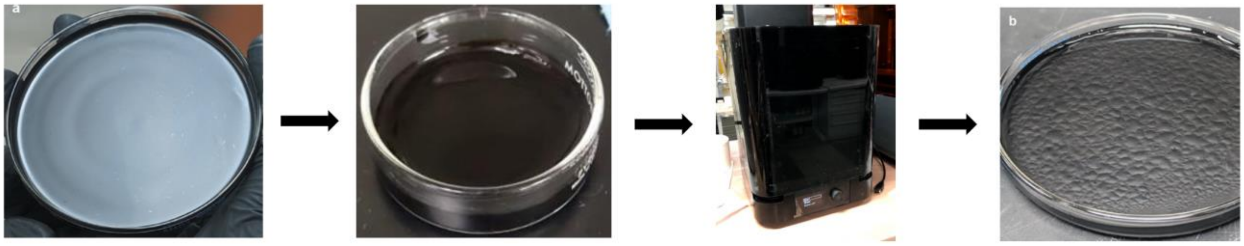

Drop-casted graphene oxide

Soaked sample with DI water and L-AA aqueous solution

NUV light irradiation (405 nm wavelength)

Removal of L-AA, followed by drying of sample overnight

Figure 3.1: Methodology of L-AA reduction of graphene oxide.

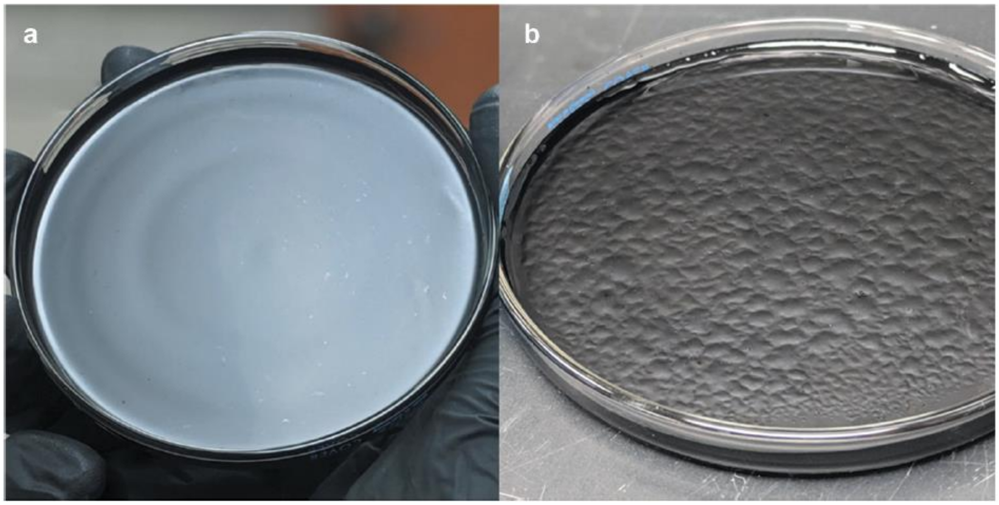

Figure 3.2: a) GO drop-casted onto quartz glass substrate, b) GO film immediately after chemical reduction through L-AA.

Results

Intercalation of water could have caused variation in the reduction of graphene oxide films. Another issue can be attributed to L-AA reduction byproducts, typically seen with green reductants. The reduction of GO films begins on the surface and slowly migrates through paths of loosely packed structures of the graphene oxide. The sample exhibiting the best reduction was the one soaked in L-AA for 48 hours and exposed to NUV for 3 hours. This sample contains an O/C ratio of 0.23 and a C-C bond concentration of 60.70%, comparable to other GO reduced by green reductants.

3.4 CONCLUSION

The use of L-ascorbic acid as a green chemical reductant with near ultraviolet light produced graphene oxide films with reduction. This reduction was characterized by scanning electron microscopy (SEM), Fourier transform infrared spectroscopy (FT-IR), wide-angle X-ray scattering (WAXS), and X-ray photoelectron spectroscopy (XPS). Characterization showed the removal of oxygen-containing functional groups [32]. Reduced graphene oxide films exhibit differences in reduction depending on the amount of exposure to L-AA. NUV-radiation at 405 nanometer wavelength accelerates the degradation of L-ascorbic acid and promotes the reduction of graphene oxide, while also increasing the depth of reduction from the surface layers to lower layers in between and throughout the film. Longer exposure to NUV-radiation produces a more uniformly reduced graphene oxide film. This research further allows the applications of reduced graphene oxide in energy storage devices, electronics, composite materials, and sensors.

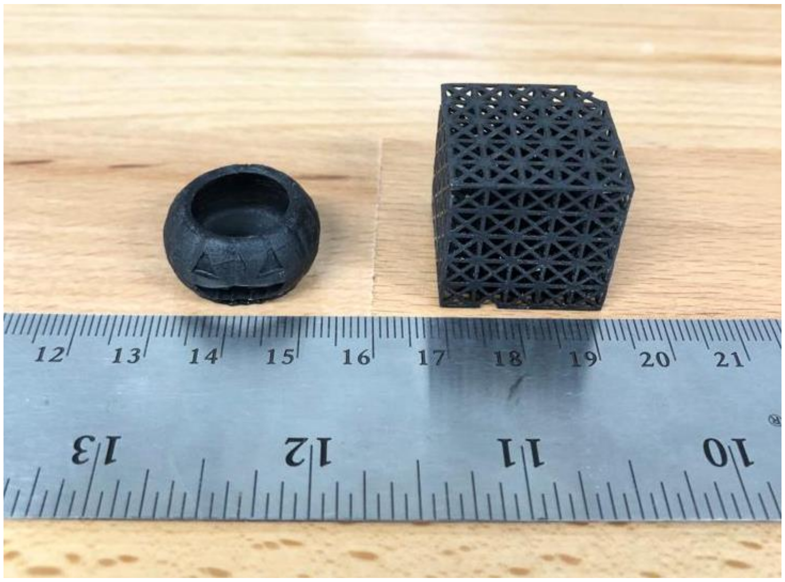

Figure 3.3: Parts 3D printed with resin containing the reduced graphene oxide produced. Parts were printed using stereolithography, a vat photopolymerization technology that uses a UV laser to cure parts.

References

[1] 14:00-17:00, “ISO/ASTM 52900:2015,” *ISO*. https://www.iso.org/cms/render/live/en/sites/isoorg/contents/data/standard/06/96/69669.html (accessed Apr. 08, 2022).

[2] M. Attaran, “The rise of 3-D printing: The advantages of additive manufacturing over traditional manufacturing,” *Business Horizons*, vol. 60, no. 5, pp. 677–688, Sep. 2017, doi: 10.1016/j.bushor.2017.05.011.

[3] S. Ford and M. Despeisse, “Additive manufacturing and sustainability: an exploratory study of the advantages and challenges,” *Journal of Cleaner Production*, vol. 137, pp. 1573–1587, Nov. 2016, doi: 10.1016/j.jclepro.2016.04.150.

[4] A. Bacciaglia, A. Ceruti, and A. Liverani, “Additive Manufacturing Challenges and Future Developments in the Next Ten Years,” in *Design Tools and Methods in Industrial Engineering*, Cham, 2020, pp. 891–902. doi: 10.1007/978-3-030-31154-4_76.

[5] O. Alabi, K. Ologbonjaye, O. Awosolu, and A. E, “Public and Environmental Health Effects of Plastic Wastes Disposal: A Review,” *Journal of Toxicology and Risk Assessment*, vol. 5, Apr. 2019, doi: 10.23937/2572-4061.1510021.

[6] M. R. Vengatesan, A. M. Varghese, and V. Mittal, “Chapter 3 - Thermal properties of thermoset polymers,” in *Thermosets (Second Edition)*, Q. Guo, Ed. Elsevier, 2018, pp. 69–114. doi: 10.1016/B978-0-08-101021-1.00003-4.

[7] F. Chu *et al.*, “Exploration on structural rules of highly efficient flame retardant unsaturated polyester resins,” *Journal of Colloid and Interface Science*, vol. 608, pp. 142–157, Feb. 2022, doi: 10.1016/j.jcis.2021.09.124.

[8] A. Das and P. Mahanwar, “A brief discussion on advances in polyurethane applications,” *Advanced Industrial and Engineering Polymer Research*, vol. 3, no. 3, pp. 93–101, Jul. 2020, doi: 10.1016/j.aiepr.2020.07.002.

[9] M. Nosaka *et al.*, “Effect of the Microstructures on Vulcanized Rubber Frictions,” *Langmuir*, vol. 37, no. 21, pp. 6459–6467, Jun. 2021, doi: 10.1021/acs.langmuir.1c00590.

[10] S. H. Teoh, Z. G. Tang, and G. W. Hastings, “Thermoplastic Polymers In Biomedical Applications: Structures, Properties and Processing,” in *Handbook of Biomaterial Properties*, J. Black and G. Hastings, Eds. Boston, MA: Springer US, 1998, pp. 270–301. doi: 10.1007/978-1-4615-5801-9_19.

[11] M. Häußler, M. Eck, D. Rothauer, and S. Mecking, “Closed-loop recycling of polyethylene-like materials,” *Nature*, vol. 590, no. 7846, Art. no. 7846, Feb. 2021, doi: 10.1038/s41586-020-03149-9.

[12] W. Zhao, C. Kumar Kundu, Z. Li, X. Li, and Z. Zhang, “Flame retardant treatments for polypropylene: Strategies and recent advances,” *Composites Part A: Applied Science and Manufacturing*, vol. 145, p. 106382, Jun. 2021, doi: 10.1016/j.compositesa.2021.106382.

[13] Y. Liu, C. Zhou, F. Li, H. Liu, and J. Yang, “Stocks and flows of polyvinyl chloride (PVC) in China: 1980-2050,” *Resources, Conservation and Recycling*, vol. 154, p. 104584, Mar. 2020, doi: 10.1016/j.resconrec.2019.104584.

[14] D. Montarnal, M. Capelot, F. Tournilhac, and L. Leibler, “Silica-Like Malleable Materials from Permanent Organic Networks,” *Science*, vol. 334, no. 6058, pp. 965–968, Nov. 2011, doi: 10.1126/science.1212648.

[15] Q. Shi *et al.*, “Recyclable 3D printing of vitrimer epoxy,” *Materials Horizons*, vol. 4, no. 4, pp. 598–607, 2017, doi: 10.1039/C7MH00043J.

[16] W. Denissen, J. M. Winne, and F. E. D. Prez, “Vitrimers: permanent organic networks with glass-like fluidity,” *Chemical Science*, vol. 7, no. 1, pp. 30–38, 2016, doi: 10.1039/C5SC02223A.

[17] B. Krishnakumar, R. V. S. P. Sanka, W. H. Binder, V. Parthasarthy, S. Rana, and N. Karak, “Vitrimers: Associative dynamic covalent adaptive networks in thermoset polymers,” *Chemical Engineering Journal*, vol. 385, p. 123820, Apr. 2020, doi: 10.1016/j.cej.2019.123820.

[18] A. Ruiz de Luzuriaga, G. Solera, I. Azcarate-Ascasua, V. Boucher, H.-J. Grande, and A. Rekondo, “Chemical control of the aromatic disulfide exchange kinetics for tailor-made epoxy vitrimers,” *Polymer*, vol. 239, p. 124457, Jan. 2022, doi: 10.1016/j.polymer.2021.124457.

[19] S. Kitagawa and R. Matsuda, “Chemistry of coordination space of porous coordination polymers,” *Coordination Chemistry Reviews*, vol. 251, no. 21, pp. 2490–2509, Nov. 2007, doi: 10.1016/j.ccr.2007.07.009.

[20] “Chemistry and Biology of Biosynthetic Diels–Alder Reactions - Stocking - 2003 - Angewandte Chemie International Edition - Wiley Online Library.” https://onlinelibrary.wiley.com/doi/full/10.1002/anie.200200534 (accessed May 08, 2022).

[21] R. Xie *et al.*, “Glass transition temperature from the chemical structure of conjugated polymers,” *Nat Commun*, vol. 11, no. 1, Art. no. 1, Feb. 2020, doi: 10.1038/s41467-020-14656-8.

[22] M. Guerre, C. Taplan, J. M. Winne, and F. E. D. Prez, “Vitrimers: directing chemical reactivity to control material properties,” *Chemical Science*, vol. 11, no. 19, pp. 4855–4870, 2020, doi: 10.1039/D0SC01069C.

[23] P. Auerkari, “Mechanical and physical properties of engineering alumina ceramics,” p. 27.

[24] P. Figiel, M. Rozmus, and B. Smuk, “Properties of alumina ceramics obtained by conventional and non-conventional methods for sintering ceramics,” *Journal of Achievements in Materials and Manufacturing Engineering*, vol. 48, no. 1, p. 6, 2011.

[25] A. J. Ruys, *Alumina Ceramics: Biomedical and Clinical Applications*. Woodhead Publishing, 2018.

[26] “Form Wash and Form Cure: Automated Post-Processing,” *Formlabs*. https://formlabs.com/post-processing/wash-cure/ (accessed May 16, 2022).

[27] “Design of lattice structure for additive manufacturing | IEEE Conference Publication | IEEE Xplore.” https://ieeexplore.ieee.org/abstract/document/7790182 (accessed Mar. 24, 2022).

[28] Q. Zeng *et al.*, “Additive manufacturing alumina components with lattice structures by digital light processing technique,” *Journal of Materials Science & Technology*, vol. 35, no. 12, pp. 2751–2755, Dec. 2019, doi: 10.1016/j.jmst.2019.08.001.

[29] M. Pelanconi *et al.*, “Application of Ceramic Lattice Structures to Design Compact, High Temperature Heat Exchangers: Material and Architecture Selection,” *Materials*, vol. 14, no. 12, Art. no. 12, Jan. 2021, doi: 10.3390/ma14123225.

[30] F. Kotz *et al.*, “Glassomer—Processing Fused Silica Glass Like a Polymer,” *Advanced Materials*, vol. 30, no. 22, p. 1707100, 2018, doi: 10.1002/adma.201707100.

[31] A. K. Geim, “Graphene: Status and Prospects,” *Science*, vol. 324, no. 5934, pp. 1530–1534, Jun. 2009, doi: 10.1126/science.1158877.

[32] J. Regis *et al.*, “Near-UV light assisted green reduction of graphene oxide films through l-ascorbic acid,” *International Journal of Smart and Nano Materials*, vol. 12, no. 1, pp. 20–35, Jan. 2021, doi: 10.1080/19475411.2021.1887396.

[33] D. R. Dreyer, S. Park, C. W. Bielawski, and R. S. Ruoff, “The chemistry of graphene oxide,” *Chem. Soc. Rev.*, vol. 39, no. 1, pp. 228–240, Dec. 2009, doi: 10.1039/B917103G.

[34] S. Park, J. An, J. R. Potts, A. Velamakanni, S. Murali, and R. S. Ruoff, “Hydrazine-reduction of graphite- and graphene oxide,” *Carbon*, vol. 49, no. 9, pp. 3019–3023, Aug. 2011, doi: 10.1016/j.carbon.2011.02.071.

[35] J. Usaga, D. C. Manns, C. I. Moraru, R. W. Worobo, and O. I. Padilla-Zakour, “Ascorbic acid and selected preservatives influence effectiveness of UV treatment of apple juice,” *LWT - Food Science and Technology*, vol. C, no. 75, pp. 9–16, 2017, doi: 10.1016/j.lwt.2016.08.037.

Glossary

Additive manufacturing: Also known as 3D printing; the process of joining materials to make parts from 3D model data, usually layer upon layer, as opposed to subtractive manufacturing and formative manufacturing methodologies

Alumina: Al2O3, a white, or nearly colorless substance derived from bauxite, an aluminum-rich clay-like material found in the Earth's crust

Ceramics: Hard materials exhibiting excellent thermal, physical and mechanical properties made by shaping and firing at high temperatures

Lattice: Two or three-dimensional micro-architectures made of networks of channels or beams with good mechanical properties and reduced weight

Lithography: Refers to the process of curing, polymerizing, parts using a light source

Material extrusion: One of the seven additive manufacturing technologies; process in which material is selectively dispensed through a nozzle or orifice

Polymers: A class of substances composed of smaller chemical units called monomers bonded together; more commonly known as plastics or resins

Vat photopolymerization: One of the seven additive manufacturing technologies; process in which liquid photopolymer in a vat is selectively cured by light-activated polymerization

Vita

Elsa Bramasco-Rivera was born in Long Beach, California. At the age of seven, she and her family moved to El Paso, TX, which she now considers her hometown. Elsa speaks fluent English and Spanish, with Spanish being her first language as a daughter of Mexican immigrants. She enrolled at the University of Texas at El Paso in Fall 2016, where she began her bachelor's degree in mechanical engineering.

As an undergraduate, she joined the Center for Advanced Materials Research Lab where she worked on metallic thin films used for electronic applications. She completed a summer internship in 2019 at the University of California - Santa Barbara Materials Research Laboratory where she continued to work on and characterize thin films. She then grew an interest in additive manufacturing and changed research groups to the Smart Materials Printing Lab, working on the synthesis and 3D printing of polymers, which makes up the first chapter of this thesis. She completed a second summer internship in 2020 at the Kansas City National Security Campus evaluating processing parameters for a femtosecond laser.

In Spring 2021, she graduated with honors with her Bachelor of Science in Mechanical Engineering and a minor in mathematics. In Summer 2021, she enrolled in the Master's Program of Mechanical Engineering. During this same summer, she completed an internship at Amazon where she worked on automated machinery. After her internship, she co-led a project on the additive manufacturing and characterization of ceramics, which makes up the second chapter of this thesis.

Elsa has co-authored one publication and has one on-going publication.

Contact Information: Elsa Bramasco-Rivera – ebramascor@miners.utep.edu